AVIAN CONSERVATION & ECOLOGY

VOLUME 18, ISSUE 2, ARTICLE 16

Dunn, E. H., K. J. Kardynal, K. M. Covino, S. R. Morris, R. L. Holberton, and K. A. Hobson. 2023. Feather isotopes (δ^2H_f) and morphometrics reveal population-specific migration patterns of the Blackpoll Warbler (*Setophaga striata*). Avian Conservation and Ecology 18(2):16. https://doi.org/10.5751/ACE-02539-180216

Research Paper

Feather isotopes (δ^2H_f) and morphometrics reveal population-specific migration patterns of the Blackpoll Warbler (*Setophaga striata*)

Erica H. Dunn [1], *Kevin J. Kardynal* [2], *Kristen M. Covino* [3,4], *Sara R. Morris* [4,5], *Rebecca L. Holberton* [6] *and Keith A. Hobson* [7,8]
[1]Canadian Migration Monitoring Network, Birds Canada, [2]Wildlife Research Division, Environment and Climate Change Canada, [3]Biology Department, Loyola Marymount University, [4]Shoals Marine Laboratory, University of New Hampshire, [5]Department of Biology, Canisius College, [6]Laboratory of Avian Biology, School of Biology and Ecology, University of Maine, [7]Environment and Climate Change Canada, [8]Department of Biology, Western University

ABSTRACT. Blackpoll Warblers (*Setophaga striata*) have declined precipitously according to the North American Breeding Bird Survey, but that survey's coverage of the boreal breeding range is limited. Migration monitoring offers an attractive tool for additional assessment because migrants from inaccessible portions of the breeding range are included in counts. However, for site-specific trends to be combined into regional or range-wide population trends, the breeding ground origin of the migrants counted at each site must be known. Blackpolls have a loop migration pattern in which spring and fall migrants follow different paths, but very little is known about population-specific routes within North America. We used stable hydrogen isotope assays of tail feathers (δ^2H_f, 4th rectrix) and wing-length measurements from migration monitoring sites across Canada and the northeastern United States to broadly delineate breeding/natal origins of blackpolls captured at those sites. Blackpolls captured on spring migration in southern Ontario and western Quebec had characteristics expected of birds from breeding range west of the Great Lakes. These birds travel northward from the eastern Gulf of Mexico to Canada east of the Great Lakes before turning westward to reach their final destination between northwestern Ontario and eastern portions of the Northwest Territories. Many birds sampled at Great Lakes sites prior to 2010, but not thereafter, had δ^2H_f and wing-length characteristics expected of breeding range in eastern Canada, suggesting differential rates of population change among regions. Estimates of migratory connectivity indicated considerable mixing of populations from different portions of the breeding range during migration. Our results both corroborate and refine the known clockwise loop migration pattern, provide new insight into spring migration routes across North America, and provide a foundation for incorporating breeding ground origins into estimations of range-wide population trends based on standardized migration counts.

Les isotopes de plumes (δ^2H_f) et la morphométrie révèlent des schémas de migration spécifiques aux populations de la Paruline rayée (*Setophaga striata*)

RÉSUMÉ. Selon le Relevé des oiseaux nicheurs d'Amérique du Nord, le nombre de Parulines rayées (*Setophaga striata*) a diminué précipitamment, mais la couverture de l'aire de nidification boréale par ce relevé est limitée. Le suivi pendant les migrations offre un outil intéressant pour une évaluation supplémentaire, car les migrateurs provenant de parties inaccessibles de l'aire de nidification sont comptés lors de ces dénombrements. Cependant, pour que la tendance spécifique à un site puisse être combinée en tendances de population régionales ou à l'échelle de l'aire de répartition, le lieu de nidification des migrateurs comptés à chaque site doit être connu. Les Parulines rayées ont un schéma de migration en boucle, dans lequel les migrateurs au printemps et à l'automne empruntent des chemins différents, mais on en sait très peu sur les itinéraires spécifiques aux populations en Amérique du Nord. Nous avons utilisé le dosage d'isotopes stables d'hydrogène de plumes de queue (δ^2H_f, 4e rectrice) et des mesures de la longueur de l'aile sur des sites de suivi de la migration au Canada et dans le nord-est des États-Unis pour déterminer de façon générale le lieu de nidification/natalité des parulines capturées à ces sites. Les parulines capturées lors de la migration printanière dans le sud de l'Ontario et l'ouest du Québec présentaient les caractéristiques attendues d'oiseaux provenant de l'aire de nidification située à l'ouest des Grands Lacs. En provenance de l'est du golfe du Mexique, ces oiseaux voyagent vers le nord jusqu'à l'est des Grands Lacs au Canada, puis bifurquent vers l'ouest pour atteindre leur destination finale entre le nord-ouest de l'Ontario et les parties est des Territoires du Nord-Ouest. De nombreux oiseaux échantillonnés sur des sites des Grands Lacs avant 2010, mais pas après, présentaient des caractéristiques de δ^2H_f et de longueur d'aile attendues dans l'aire de nidification de l'est du Canada, indiquant des taux différentiels de changement de population entre les régions. L'évaluation de la connectivité de migration montre un mélange important de populations provenant de différentes parties de l'aire de nidification pendant la migration. Nos résultats corroborent et améliorent le modèle connu de migration en boucle dans le sens des aiguilles d'une montre, donnent une nouvelle perspective des itinéraires de migration printanière en Amérique du Nord et fournissent une base pour l'incorporation de l'origine de nidification dans l'estimation de la tendance de la population à l'échelle de l'aire de répartition, basée sur des dénombrements normalisés réalisés pendant les migrations.

Key Words: *deuterium, loop migration, migratory connectivity, stable isotopes, wing length*

Corresponding author: Erica H Dunn, EricaHDunn@gmail.com

INTRODUCTION

Knowledge of the degree of connectivity between breeding and wintering areas contributes to understanding the ecology and evolution of migratory species and is also crucial to effective conservation (Webster and Marra 2005). Because variation in population trajectories can result from factors affecting populations during any stage of the annual cycle, appropriate direction of conservation action depends also on knowing the population-specific migration routes that link breeding and wintering areas.

Migration pathways can be determined by tracking individual birds using, for example, band recoveries, global positioning systems (GPS), light-sensitive geolocator devices, or radio telemetry methods, although results from tracking individuals are biased toward locations where migrants are most likely to be captured and/or detected (Cohen et al. 2014). Further, maps of results from tracked individuals typically connect start and end locations using straight or great circle lines that represent the shortest pathway between them (e.g., DeLuca et al. 2019) even though migrants do not always follow shortest routes or use the same routes during both migration seasons (Ruegg and Smith 2002, Schmaljohann et al. 2012, Holberton et al. 2015, 2019).

An efficient approach to determining broad migration pathways for all segments of a species' population is to use intrinsic markers to infer previous molt or breeding location of entire groups of birds intercepted at various stages of the annual cycle. Such markers include genetic information (Ruegg et al. 2014, Bazzi et al. 2016) and naturally occurring stable isotope ratios that integrate local food web or environmental isotope values into growing inert tissues (Hobson and Wassenaar 2019). Flight feathers (wing and tail) are often used for stable hydrogen isotope assay for species that grow their feathers on or close to the breeding grounds prior to fall migration. Both adults and young of the year retain these feathers until molting them a year later. Spatially explicit approaches have been developed to assign individuals probabilistically to the likely portion of the breeding range where those feathers were grown (Hobson et al. 2012, 2019) making it possible to delimit the most probable breeding or natal regions of the previous year for birds captured at any time within the non-breeding season (Hobson et al. 2015, Cardenas-Ortiz et al. 2021, Franzoi et al. 2021). Additional clues as to breeding ground origin may come from morphometric features that vary across a species' range. For example, wing length and shape are often correlated with migration distance and have been used previously by researchers interested in migratory connectivity (Delingat et al. 2011, Rushing et al. 2014, Ożarowska et al. 2021). Both isotopic and morphometric techniques can broadly identify probable breeding ground origins at continental scales, providing context for results from individual tracking.

We use these techniques to refine our knowledge of migration routes followed within North America by the Blackpoll Warbler (*Setophaga striata*, hereafter blackpoll). Fall migrants are known to move to Atlantic coastal areas of Canada and the northeastern United States before making overwater flights to South America, whereas returning spring migrants enter North America via the Florida peninsula and the eastern U.S. Gulf Coast before proceeding overland to breeding destinations (DeLuca et al. 2015, 2019, 2020; Holberton et al. 2015, 2019; Morris et al. 2016, Covino et al. 2020). Despite this loop migration pattern being well documented, however, little is known about the seasonal pathways followed by birds from different parts of the breeding range as they move across the continent.

Conservation concern for blackpolls makes it important to learn more about population-specific migration routes. According to the North American Breeding Bird Survey (BBS), blackpolls have declined more than 75% since 1970 (Sauer et al. 2020, Smith et al. 2023). However, most of the blackpoll breeding range is poorly sampled by the BBS, so population-level trend estimates have low certainty (Environment and Climate Change Canada [ECCC] 2019). Migration count data are recognized as a valuable alternative source for trend estimation because individuals from all portions of the range are accessible for counting (Dunn et al. 2005, Crewe et al. 2008, Canadian Migration Monitoring Network 2021). However, migration counts are of limited value for assessing range-wide population trends unless the breeding/natal origins of migrants recorded at each count site are known.

We used feather stable hydrogen isotope assays and wing morphometrics to identify probable breeding or natal regions of blackpolls captured at migration stopover sites spanning North America (Fig. 1) and calculated the strength of migratory connectivity between derived breeding/natal origins and sampling locations during the spring and fall migration seasons. Identifying the source breeding grounds of birds counted at specific long-term monitoring sites will facilitate combining of site-specific migration counts into regional and range-wide trend estimates.

Fig. 1. δ^2H_f isoscape for the breeding range of the Blackpoll Warbler (*Setophaga striata*). Red lines separate the three breeding/natal regions defined for this study. Triangles show sites of feather collection for stable isotope analysis and dots indicate locations contributing wing-length data. (See Appendix 1 for details.) The dashed line at −90°W longitude marks the division between east and west used for certain analyses of wing length (Table 1).

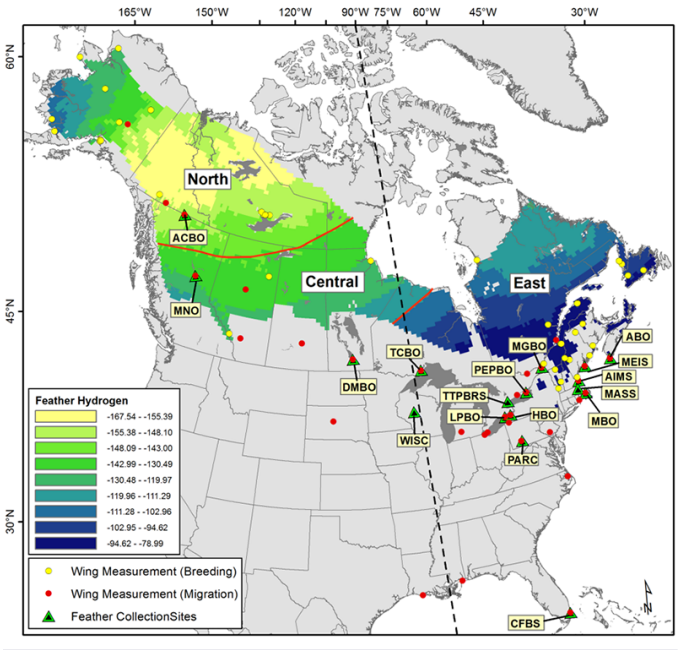

METHODS

Feather stable isotope analyses

Stable hydrogen isotope ratios in tail feathers indicate where those feathers were grown, which in blackpolls takes place at or near the area where the birds bred or were raised (DeLuca et al. 2020). One or both fourth rectrix feathers (R4) were collected from migrating blackpolls through a cooperative network of migration monitoring stations (Canadian Migration Monitoring Network 2021). Feathers were stored in paper envelopes at room temperature until preparation for stable hydrogen isotope assay either at the ECCC stable isotope laboratory in Saskatoon or at the LSIS-AFAR stable isotope facility at the University of Western Ontario. The d^2H protocols for feathers were the same in both laboratories (coordinated by KAH). Importantly, both labs used the same (keratin) calibration standards. The distal vane portion of each feather sample was soaked for > 5 h in 2:1 chloroform:methanol solution, then rinsed with fresh solvent and dried in a fume hood for 48 h (Wassenaar 2019). Dried samples were weighed (350 ± 10 µg) into silver capsules and crushed. At the ECCC laboratory, samples were loaded into a zero blank autosampler under helium (He) flow and combusted pyrolytically using a glassy carbon reactor at 1350 °C in a Eurovector 3000 elemental analyzer (Milan, Italy). Hydrogen gas (H_2) was analyzed isotopically in an interfaced Isoprime mass spectrometer (Crewe, UK). The process was generally the same at the LSIS-AFAR laboratory, but samples were first loaded into a Uni-Prep carousel (Eurovector, Milan, Italy) heated to 60 °C, evacuated and flushed with dry He gas, and held under pressure before being combusted at 1350 °C on glassy carbon also in a Eurovector elemental analyzer interfaced with a Thermo Delta V Plus isotope ratio mass spectrometer (Thermo, Bremen, Germany). Within analytical runs, keratin reference standards CBS (Caribou Hoof: −197 per mil) and KHS (Kudu Horn: −54.1 per mil) were used to calibrate samples. All results are reported for non-exchangeable hydrogen (H), expressed in the typical delta (δ) notation, in units of per mil (‰) and normalized on the Vienna Standard Mean Ocean Water (VSMOW) scale using the comparative equilibration approach of Wassenaar and Hobson (2003). Based on within-run replicate (n = 5) measurements of laboratory keratin standards, we estimated measurement precision for both laboratories to be ± 2‰.

To supplement our assays, we compiled individual δ^2H_f values from the authors of previously published stable isotope analyses of blackpolls (Dunn et al. 2006; Holberton et al. 2015, 2019; Ma et al. 2018) and included them in our study (sites shown in Fig. 1). All these studies involved KAH as a co-author, and all δ^2H_f assays were conducted at the same laboratories using the same methods and with extensive inter-laboratory checks.

Wing length

Geographic variation in wing length of migrating blackpolls has previously been demonstrated using large data sets (Morris et al. 2016, Covino et al. 2020). We combined data contributed to those two publications with additional migration samples and with data collected at breeding sites (Fig. 1, Appendices 1 and 2). We classified birds as breeders if they were captured within the breeding range between 1 June and 15 August. Otherwise, we considered individuals to be spring migrants if captured from first arrival–15 June and as fall migrants if captured from 16 August–15 November. Measurements taken outside these date ranges were omitted from analyses.

Unflattened wing chords (Ralph et al. 1993) were measured to the nearest 0.5 or 1 mm, depending on site. Age and sex were determined using plumage characteristics (Pyle 1997, Piranga 2021). Wing length differs by sex (Appendix 3, Fig. A3.1), and sexing by plumage is straightforward during spring migration and the breeding season. However, it is difficult to determine sex during fall migration, particularly for young-of-the-year (hatch year, HY). Similarly, it is relatively easy to separate HY blackpolls from adults (after hatch-year, AHY) during fall migration but more difficult in spring to distinguish one-year-old birds (second year, SY) from older birds (after second-year, ASY). Moreover, data from different cooperators varied widely in the proportions of imprecisely aged or sexed individuals and are likely biased toward the age/sex groups most easily recognized in each season (Morris et al. 2016, Covino et al. 2020). To avoid such biases in analyses of wing length of migrants we excluded all data from HY birds captured in fall and combined data for adults in each season without regard to sex. Sex was considered only in our discriminant function analyses of breeding birds. Mean wing lengths are presented with standard errors, and samples were compared using non-parametric methods (Mann-Whitney U test or Kruskal-Wallis H test; SigmaStat 4.0).

Identifying probable breeding/natal origin

We arbitrarily divided the blackpoll breeding range into three regions based on the continental pattern of δ^2H_f values (Fig. 1): North ($\delta^2H_f \leq -143$‰), Central ($\delta^2H_f = -112$ to -142‰) and East ($\delta^2H_f \geq -111$‰). The border between Central and East Regions separates portions of the breeding range to the west and east of the Great Lakes longitudinally, whereas the border between North and Central Regions splits the area west of the Great Lakes approximately by latitude. Hereafter we capitalize "Region" when referring to these pre-defined portions of the breeding range.

We tested the potential use of wing length from breeding-ground samples as a means of assigning adults to one of these three breeding range Regions, using linear discriminant analysis (LDA) with wing length and sex as predictors. We used 30% of the data to train the LDA and the remainder of the data to assess the fit of the model. LDA was conducted with the MASS package (Venables and Ripley 2002) in the R computing environment (R Core Team 2022). The LDA with wing length and sex used to predict Region of origin had an overall accuracy of 73.8%; however, some sex data were missing, and no birds were assigned to the Central Region, indicating that the model could not differentiate between the North and Central Regions. Prediction accuracy with sex excluded fell to 62%.

Using δ^2H_f results, we assigned probable breeding/natal Region of blackpolls captured during migration with a spatially explicit likelihood assignment method described elsewhere (Wunder 2010, Van Wilgenburg and Hobson 2011, Smith et al. 2019). We extracted site-specific predicted amount-weighted mean precipitation δ^2H values (δ^2H_p) based primarily on the long-term dataset provided by the Global Network of Isotopes in

Precipitation (GNIP) of the International Atomic Energy Agency (https://www.iaea.org/services/networks/gnip) as depicted in the Bowen et al. (2005) δ^2H_p isoscape (~0.33' × 0.33' resolution). We then modeled the relationship of those data with δ^2H_f values from breeding long-distance canopy foraging insectivorous birds (Hobson et al. 2012) augmented with blackpoll δ^2H_f samples from the breeding grounds (Holberton et al. 2015, 2019) using 1000 non-parametric bootstrap regressions containing 2/3 of the known-source birds randomly selected with replacement. This resulted in a mean precipitation to feather isoscape rescaling function relating δ^2H_p to δ^2H_f of: $\delta^2H_f = -37.30\ (\pm\ 11.56) + 0.81\ (\pm\ 0.15) * \delta^2H_p$. We then cropped the δ^2H_f isoscapes to the digital breeding range for the Blackpoll Warbler (BirdLife International and Nature Serve 2014). We determined the variance between each of the separately derived calibrated isoscapes from the bootstrapped regressions to obtain a single surface depicting the variance (σ^2) of the rescaled isoscapes. The mean residual variance from the regressions was used to represent inter-individual variance ($\sigma^2_{individual}$) and we created a spatially explicit prediction error surface (Vander Zanden et al. 2014) to incorporate error in the assignments.

$$\sqrt{\sigma^2_{rescale} + \sigma^2_{individual}} \quad (1)$$

We subsequently applied a normal probability density function (PDF) to derive estimates of the likelihood that a given pixel within the calibrated δ^2H_f isoscape represented a potential growth site for a given feather in our sample by comparing δ^2H_f against model predicted δ^2H_f within each pixel. Predicted δ^2H_f values were treated as the means in the PDF, against which individual δ^2H_f sample values were compared, and these values were used in the derived spatially explicit prediction error surface as the estimate of variance in the PDF. Spatially explicit likelihoods for cells were subsequently reclassified into a binary surface using a 2:1 odds ratio, where cells in the upper 67% of estimated likelihoods were retained as likely (1) versus unlikely (0) origins for each sample for mapping. Individual birds were assigned to multiple potential origins (i.e., cells) within the isoscape using this approach because of the underlying regional similarity and spatial autocorrelation of individual cells in the isoscape. Results of individual assignment analyses were then summed across assignments for all individuals for each station, year, and season combination. Spatial representations of potential origins for the given sample corresponded then to the number of individuals assigned spatially. We used zonal statistics (mean of values within each Region) on individual likelihood surfaces to determine which Region each bird likely originated from. To assess the degree of uncertainty in these assignments we used bootstrapping to resample the assignment results 1000 times. CIs were small (Appendix 3, Fig. A3.2), as expected given that the Regions were defined based on δ^2H_f values. We edited digital files and assigned origins using packages in the R version 4.0.3 computing environment as follows: raster (Hijmans 2023), maptools (Bivand and Lewin-Koh 2021), car (Fox and Weisberg 2019), rgdal (Bivand et al. 2023), and rgeos (Bivand and Rundel 2021).

We also conducted a separate set of isotope assignments to probable Region of origin that included the posterior probabilities from the wing length LDA for breeding adults as a Bayesian prior. Samples without sex information (43% of cases) were given the same prior (0.33) across all Regions. Predictive accuracy of Regional assignment was lower than when based on δ^2H_f values alone, largely because of the high degree of overlap in wing length among the three Regions (Appendix 3, Fig. A3.1). The effect on mapped results was modest in most cases (Appendix 3, Figs. A3.3 and A3.4)

Migratory connectivity

We used stable isotope results to estimate the strength of migratory connectivity (MC) of Blackpoll Warblers, to determine the degree to which populations from different portions of the breeding range co-occur during migration. To accomplish this, we used the methods in the MigConnectivity v.0.4.1.9 R package (Hostetler and Hallworth 2023), which accounts for variation in sampling effort and can incorporate different types of tracking data, including stable isotopes. Using this approach, values of MC range from −1 to 1, but are typically > 0. Lower values indicate weak connectivity with individuals from all breeding regions mixing uniformly on the non-breeding grounds, and higher values indicate strong connectivity with population-specific movement (i.e., limited mixing) between periods of the annual cycle (Cohen et al. 2014).

We estimated the strength of MC between the three Regions of the breeding range (Fig. 1) and four groups of migration monitoring sites. The latter were defined using our individual assignment probability rasters for each season to group spring and fall migration capture sites based on their geographic proximity, namely west (W; n = 1 sampling station in Yukon), central/west Great Lakes (WGL; n = 3; −98° to −84° longitude), east Great Lakes (EGL; n = 5; −84° to −74° longitude) and east (E; n = 8), with the approximate centroid coordinates of these locations used for the MC calculation. We quantified MC separately for spring and fall migration seasons to account for differences in migration routes for each period. MC estimation requires calculation of transition probabilities or the population-specific variation in movement between breeding and sampling regions. We included the mean of an index of blackpoll abundance in each of the capture regions (representing mean number of captures per day from 1999–2015) as the measure of relative abundance separately for spring and fall migration for stations where these data were available. Transition probabilities and strength of migratory connectivity were estimated using 1000 bootstrapped samples. Between season estimates of MC were contrasted using the diffStrength function (Hostetler and Hallworth 2023).

RESULTS

Probable breeding/natal origins of blackpolls captured at different migration sites in fall and spring are shown in Figs. 2 and 3. As a result of the underlying pattern in precipitation δ^2H, individual feather values are assigned to map pixels that cover large geographic areas. Bootstrapping of assignments nonetheless showed good consistency in the Region of probable origin to which each sample was assigned (Appendix 3, Fig. A3.2). Fig. 4 shows the proportion of birds from each migration site and season that were assigned to each breeding Region, providing a summary overview of all stable isotope results.

Fig. 2. Geographic distribution of assigned breeding or natal origins of Blackpoll Warblers (*Setophaga striata*) sampled during fall migration based on δ^2H_f values. Red lines show the borders between the North, Central, and East Regions (Fig. 1). The legend indicates probability from 0 to 1 (at top) that samples from the collection sites (indicated with red triangles) are isotopically consistent with a pixel of that color on the map. Maps are arranged from west to east, with (n samples) following site name: A = Delta Marsh Bird Observatory (6), B = Wisconsin (8), C = Thunder Cape Bird Observatory (TCBO) in 1999 (21), D = TCBO in 2007 (38), E = Long Point Bird Observatory (LPBO) in 2000 (13), F = LPBO in 2001 (30), G) = LPBO in 2014 (38), H = Powdermill Avian Research Center (54), I = Tommy Thompson Park Bird Research Station (15), J = Massachusetts (28), K = Manomet Bird Observatory (60), and L = Metinic Island (41).

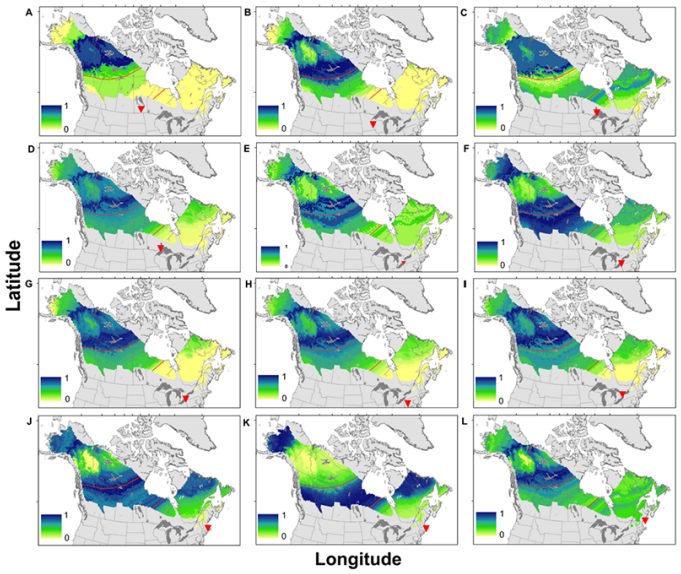

Fig. 3. Geographic distribution of assigned breeding or natal origins of Blackpoll Warblers (*Setophaga striata*) sampled during spring migration based on δ^2H_f values. Red lines show the borders between the North, Central, and East Regions (Fig. 1). The legend indicates probability from 0 to 1 (at top) that samples from the collection sites (indicated with red triangles) are isotopically consistent with a pixel of that color on the map. Maps are arranged from west to east, with n samples following site name: A = Albert Creek Bird Observatory (25), B = Long Point Bird Observatory (LPBO) in 2001 (11), C = LPBO in 2007 (20), D = LPBO in 2015 (24), E = Haldimand Bird Observatory (10), F = Tommy Thompson Park Bird Research Station (8), G = Prince Edward Point Bird Observatory (25), H = McGill Bird Observatory (9), I = Appledore Island Migration Station (23), and J = Metinic Island (25).

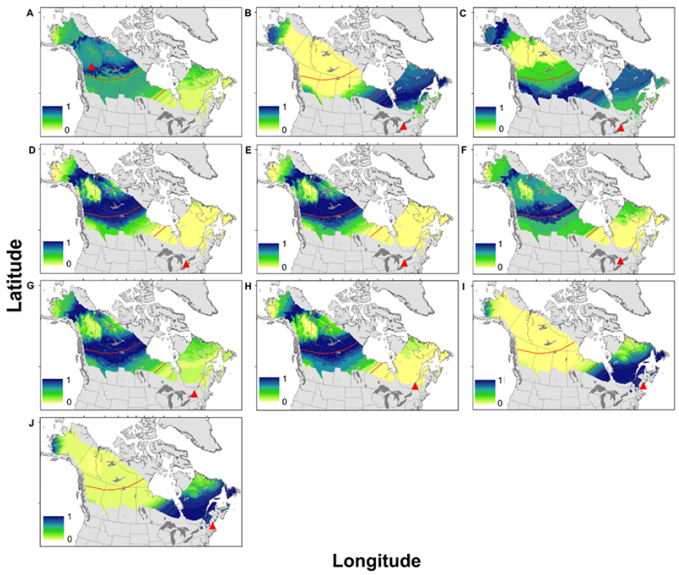

Stable hydrogen isotope values for birds captured during fall migration at far western sites (to the left of the solid vertical line in Fig. 4A) indicate that their tail feathers were grown primarily in the North Region of the breeding range (Fig. 1). Birds captured at sites in the Great Lakes region (between the vertical lines in Fig. 4A) grew feathers primarily in the North and Central Regions, except for a small proportion of birds at TCBO (NW Ontario) and LPBO (SW Ontario) that had δ^2H_f values typical of the East Region but are also indicative of western Alaska (Fig. 1). At both of these sites, the proportion of putative East Region birds declined over the years sampled; at TCBO from 32% in 1999 to 3% in 2007 and at LPBO from 21% in 2000 to 13% in 2001 and to 0% in 2014. Assignment to origin depictions suggest northwestward shifts over time in the portions of breeding range being sampled both at TCBO (Fig. 2C–D) and LPBO (Fig. 2E–G), contrary to what would be expected if the blackpolls with East Region isotope values had come from Alaska. Except for the pre-2007 samples from TCBO and LPBO, East Region blackpolls in fall were captured primarily at sites in New England (Fig. 4A).

Spring sampling locations were less broadly distributed geographically than were fall samples (Fig. 4B). The only feathers for spring migrants sampled west of the Great Lakes were from a location well within the North Region (ACBO in Yukon), and we assume that birds captured there with δ^2H_f values ascribed to Central or East Region were certain to have bred or been raised the previous summer in parts of Yukon and Alaska where those δ^2H_f values can also be found (Fig. 3A; see also variation in wing length). Spring captures at sites between the longitudes of the Great Lakes and New England (between the vertical lines in Fig. 4B) were mostly birds with δ^2H_f values that could be found on either side of the border between the North and Central Regions (Fig. 3D–H). Relatively few spring-captured blackpolls at these sites had δ^2H_f values indicating likely origin from the East Region, except for substantial proportions in the earliest samples from LPBO (Fig. 4B). As was true for fall samples, the proportion of East Region birds at LPBO in spring shifted over time: from 100% in 2001 to 60% in 2007 and to 0% in 2015. Again, the assignment depictions clearly illustrate a shift in catchment area toward the northwest (Fig. 3B–D). Other than these early samples from LPBO, East Region blackpolls were recorded almost exclusively at the two sites in New England (Fig. 4B and Fig. 3I–J).

Wing length of breeding blackpolls varied geographically (Table 1). Median wing length of birds breeding west of −90° W was 3 mm longer than for birds breeding further east (Mann-Whitney $U_{(4251101)}$

Fig. 4. Mean number of bootstrapped δ^2H_f values assigned to the North, Central, and East Regions (see Fig. 1). Bars with colored hatching are proportions from Dunn et al. (2006), for which original values were unavailable for bootstrapping. Where proportions changed over time, earlier results are shown by bars shaded in gray (North = dark gray, Central = light gray, East = white). Sites on the *x*-axis are listed from west to east and are vertically aligned between fall migration (A) and spring migration. (B) Sites to the left of the solid vertical line are situated west of Lake Superior and those to the right of the dashed line are in New England or the Maritime provinces. See Appendix 1 for key to site codes.

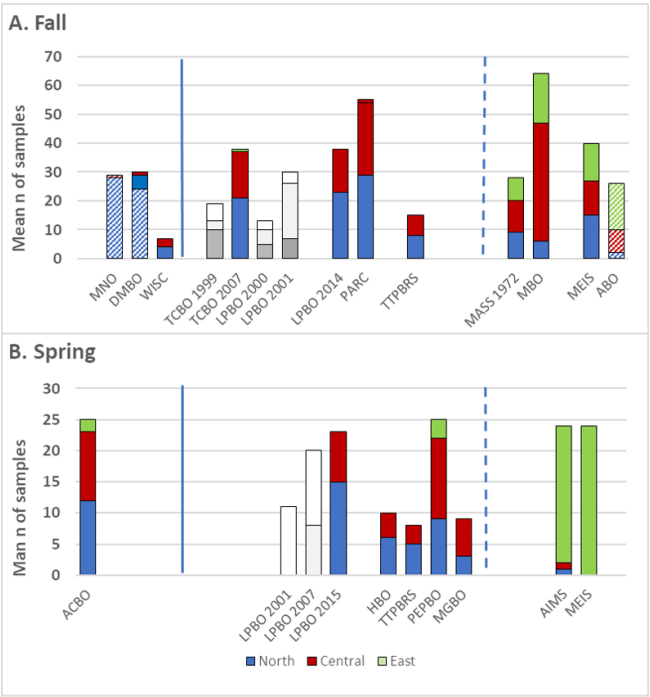

= 118064, P < 0.001). In addition, median wing of breeders in the North Region was 1 mm longer than for birds breeding in the Central Region (Mann-Whitney $U_{(347,239)}$ = 32652, P < 0.001). Despite extensive overlap of wing length among Regions (Appendix 3, Fig. A3.1), the geographic pattern of variation helped identify probable origin of migrating blackpolls that had δ^2H_f values found both in Alaska and in areas east of the Great Lakes (Fig. 1). For example, mean wing length of adults at ACBO (Yukon) in spring was 74.2 ± 0.1 mm (n = 374), indicating that the many individuals captured there with δ^2H_f values found both in Alaska and in areas east of the Great Lakes (Fig. 4) actually grew their feathers in Alaska. In contrast, mean wing length of adults captured at LPBO in spring that had δ^2H_f values used to define the East Region was 71.5 ± 0.6 mm (n = 20), typical of birds that bred east of −90° (Table 1).

Wing lengths of birds captured west of the Great Lakes did not differ according to migration season of capture (Table 1; Kruskal-Wallis H = 1.71, df = 2, P = 0.42; Fig. 5). Seasonal mean wing lengths of migrants captured in the east, however, were longer than mean wing lengths of birds breeding at the same longitudinal

Table 1. Wing chord (mm ± SE) of adult Blackpoll Warblers (*Setophaga striata*) captured west or east of the Great Lakes (−90° W) as breeders or as migrants (after hatch year, sexes combined).

Longitude		Breeders	Fall migrants	Spring migrants
West of −90° W	Mean	73.2 ± 0.1	73.1 ± 0.1	73.3 ± 0.2
	n	425	740	2053
East of −90° W	Mean	70.7 ± 0.2	72.6 ± 0.0	71.1 ± 0.0
	n	1101	14,564	9936

zones by 0.4 mm in spring and 1.9 mm in fall (Table 1; all seasonal pairwise differences significant: Kruskal-Wallis H = 1750.6, df = 2, P < 0.001). A comparison of fall vs. spring wing length restricted to sites where migrant blackpolls were measured in both seasons showed a similar pattern (Fig. 6). Differences between seasonal means in wing length at these sites were minor for most samples collected west of the Great Lakes but were > 0.5 mm longer in fall than in spring for captures farther east, a geographic pattern in agreement with the stable isotope results showing western origin birds migrating through northeastern North America.

Migratory connectivity (MC) transition probabilities differed by season. Spring transition values between birds captured in the migration corridor EGL and the North and Central breeding Regions were low (0.13–0.14), indicating considerable mixing, but high (0.73) between EGL migrants and the East breeding Region (Table 2). Transition probabilities for birds captured in both W and WGL capture regions were highest for birds moving to the North Region but indicated mixing with birds headed to Central and East Regions (although the latter includes any birds moving to parts of Alaska where the same δ^2H_f values are expected). Fall transition probabilities revealed mixing of populations from all breeding Regions across all capture sites, but the probability estimate indicating presence of East region birds among those captured at the single site in Yukon (capture region W) was likely caused by the presence of Alaskan birds with δ^2H_f values consistent with those expected for the East. Estimates of MC among the three breeding Regions and the three capture group locations indicated weak MC during migration both in spring (mean = 0.14; SE ± 0.05; 95% CI: 0.05 to 0.25) and in fall (mean = 0.04; SE ± 0.03; 95% CI: −0.01 to 0.10). The mean difference in MC estimates between spring and fall migration was 0.04 (SE ± 0.06; 95% CI: −0.006 to 0.23).

DISCUSSION

Fall migration

Fall migration routes incorporating the authors' interpretation of all available results (Fig. 7A) are essentially the same as those depicted in Holberton et al. (2015). Blackpolls from breeding areas west of the Great Lakes pass southeastward in fall across or to the north of those lakes, reaching the Atlantic coast roughly between New England and Maryland prior to initiating over-ocean flight to South America. Birds departing from breeding areas east of the Great Lakes tend to reach the coast farther to the north, in northern New England and eastern Canada. In the present study, most blackpolls captured in fall at the westernmost δ^2H_f sample sites in British Columbia (MNO) and Manitoba (DMBO) had grown their tail feathers in the North Region (Fig.

Fig. 5. Mean wing length of after-hatch-year (AHY) Blackpoll Warblers (*Setophaga striata*) at each site where n > 10, according to season and longitude, with regression (dashed line) fit to location means for breeding birds. (Details in Appendix 1.) The vertical line (−90°W, close to the western end of Lake Superior) is roughly the longitude separating the East Region from western Canada.

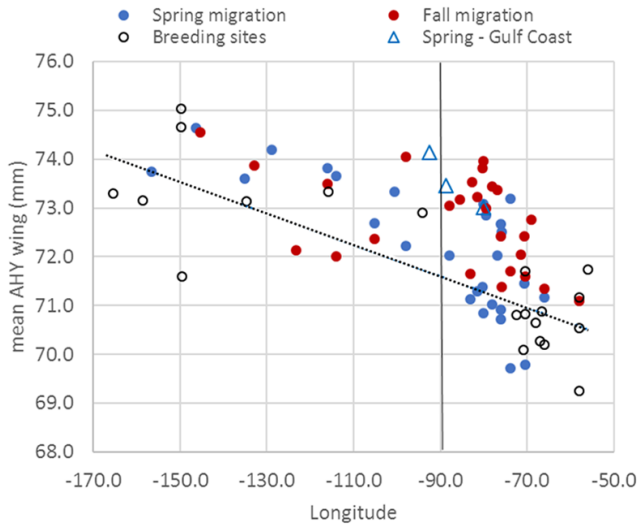

Fig. 6. Difference in mean wing chord of adult Blackpoll Warblers (*Setophaga striata*) between fall and spring migration at sites with data from both seasons. YKBO combines data from sister sites (ACBO and TLBBS) operating in different seasons. The dashed line at −90°W longitude marks the division between east and west used for certain wing length analyses (Table 1).

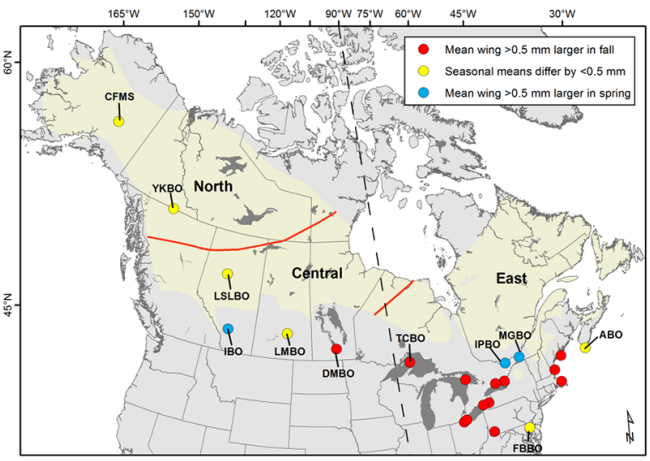

4A), with probable breeding grounds centered in Yukon (e.g., Fig. 2A). Sites in Ontario had a more equal mix of Central and North Region birds, with the highest concentrations of probable breeding origin in eastern Northwest Territories and the northern Prairie Provinces (e.g., Fig. 2F). Most of the fall migration capture sites on the east coast sampled a mix of populations from all three Regions (Fig. 2J–L; see also Smetzer and King 2020), in keeping with their locations within the fall routes proposed for blackpolls from breeding ranges west of the Great Lakes (Fig. 7A).

Patterns of wing-length variation further illustrate the strong easterly component in fall migration routes (Figs. 5 and 6). Some variation in seasonal wing length is expected based on factors other than geographical trends in wing structure, such as overwinter feather wear (Flinks and Salewski 2012) and variation in wing chord by age and sex (Morris et al. 2016; Appendix 3, Fig. A3.1). We excluded sex as a factor contributing to wing-length variation in our analyses for migrants (Morris et al. 2016), but at least in spring there was no apparent geographic pattern in sex ratio at migration capture stations (Covino et al. 2020). Moreover, if the differences we found in fall vs. spring wing lengths of migrants (Table 1) resulted largely from variation due to age composition of samples, feather wear or measurement error, we would expect similar seasonal differences at all capture sites. Because we found no such differences among blackpolls captured west of the Great Lakes (Table 1), where all migrants are assumed to have bred or been raised in western areas, we are confident that the continental pattern in wing length (Figs. 5 and 6) primarily reflects seasonal differences in the proportions of western birds traveling through eastern North America during fall and spring migration.

Wing-length patterns also provide new insight into population-specific fall migration routes. At a capture site in Alberta (IBO) that lies south of the blackpoll breeding range (Fig. 6), mean wing length was 0.6 mm shorter in fall than in spring, suggesting an eastward component to the fall migration path that causes longer-winged blackpolls from the North Region to bypass IBO further north. Among sites west of the Great Lakes, only DMBO (Manitoba) captured higher proportions of long-winged birds in fall relative to spring, but from DMBO eastward this was the usual pattern, seen at all locations in southwestern Ontario, western Pennsylvania, south shores of Lakes Erie and Ontario, and the Atlantic coast in New England (Fig. 6). Of the four sites situated east of the Great Lakes where fall-captured birds were not longer-winged than migrants captured in spring, three were among our sample sites farthest to the north and east (IPBO and MGBO, close to Ontario-Quebec border, and ABO in Nova Scotia), suggesting that the bulk of fall migrants from the North and Central Regions may bypass those capture sites to their south. Of all eastern capture locations, ABO had the highest proportion of fall migrants with East Region isotope values (Dunn et al. 2006; Fig. 4A), and wing lengths were typical of eastern breeders (Table 1) in both seasons: 71.3 mm (n = 469) in fall and 71.2 mm (n = 197) in spring. Combined with the relatively low proportions of East Region birds at other capture sites, the ABO results point to breeders from Quebec and the Maritime provinces initiating trans-Gulf migration in fall from farther north on the Atlantic Coast than do blackpolls of western origin.

Spring migration

Spring migration routes of blackpolls through North America were little known prior to this study. Based on stable isotope assay of spring migrants captured in Florida (Holberton et al. 2015, 2019) and wing lengths from birds captured on the Gulf Coast

Table 2. Mean (SE; 95% CIs) transition probabilities of Blackpoll Warbler (*Setophaga striata*) movement between three breeding ground Regions (Fig. 1) and groups of migration capture sites (defined in Methods). Bootstrapped values indicate the probability that birds captured within a migration sampling zone had grown feathers the previous summer in a given breeding ground Region. Sampling zones are W (Yukon, n = 1); WGL (west of Great Lakes, n = 3); EGL (east of Great Lakes, n = 5); E (coastal Canada and United States, n = 8).

			North	Central	East
Spring	Transition from	W	0.60 (0.10; 0.39–0.80)	0.25 (0.09; 0.09–0.44)	0.15 (0.07; 0.03–0.31)
	capture region	WGL	0.51 (0.05; 0.41–0.60)	0.28 (0.04; 0.20–0.36)	0.21 (0.04; 0.14–0.29)
	to breeding Region	EGL	0.14 (0.05; 0.05–0.25)	0.13 (0.05; 0.04–0.23)	0.73 (0.06; 0.60–0.85)
			WGL	EGL	E
Fall	Transition from	North	0.64 (0.05; 0.53–0.75)	0.62 (0.42; 0.54–0.70)	0.44 (0.04; 0.21–0.37)
	breeding Region	Central	0.25 (0.05; 0.15–0.34)	0.27 (0.04; 0.20–0.34)	0.28 (0.04; 0.06–0.16)
	to capture region	East	0.12 (0.04; 0.05–0.20)	0.11 (0.02; 0.06–0.16)	0.29 (0.04; 0.22–0.37)

Fig. 7. Proposed migration paths of the Blackpoll Warblers (*Setophaga striata*) based on the authors' interpretation of all data covered in this paper. Orange = breeding range, yellow = range during migration, blue = overwintering (DeLuca et al. 2020). The dashed line in Part A indicates the approximate southern boundary of the fall migration range (Fink et al. 2022).

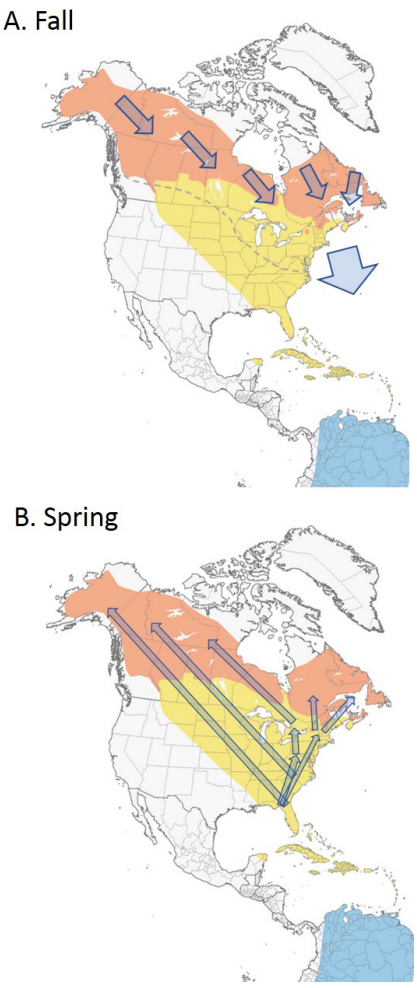

(Covino et al. 2020; Fig. 5), it was known that spring migrants bound for the westernmost parts of the breeding range start to diverge from eastbound birds by the time they reach the U.S. coastline. The only other spring δ^2H_f data available, however, were from two islands on the New England coast, which provided no hints as to migration patterns through the interior eastern United States. Spring results from this study fill in some geographic gaps and indicate substantial movement of west-bound blackpolls through areas east of the Great Lakes, only turning westward when close to Canada (Fig. 7B).

Stable hydrogen isotope data from spring capture sites in Ontario and western Quebec, spanning an east-west distance between −73° and −81°W of over 600 km, indicate that most migrants passing through that longitudinal zone bred or were raised the previous year in the Central and North Regions (Fig. 4B). Mean wing chord at several migration capture sites between these longitudes exceeded the average for blackpolls breeding in the east (Fig. 5, Table 1), including at FBBO (Maryland), PARC (Pennsylvania), HBO (Ontario), and two sites close to the Ontario-Quebec border, IPBO and MGBO. Taken together, wing length and δ^2H_f results indicate that many blackpolls with breeding origins west of the Great Lakes, likely from the eastern portions of the North and Central Regions, proceed northward in spring from Florida toward the eastern Great Lakes before changing course toward the northwest (Fig. 7B).

Migratory connectivity derived from δ^2H_f was low for both spring and fall migration, as expected given the patterns of migration. Fall movement of all blackpolls toward the Atlantic Coast leads to extensive mixing of birds from all parts of the range, and North Region birds cannot avoid passing through the Central Region during both migration seasons. As well, the relatively high probability of mixing between East and North Region birds reflects the similarity of isotope values in parts of those regions (Fig. 1). Because of population mixing en route, additional study is needed to estimate strength of connectivity between portions of the breeding range and specific parts of the non-breeding range in Latin America. Nonetheless, our results are the first quantitative estimates of migratory connectivity for blackpolls and point to the value of using stable isotopes in similar analyses for other species.

The spring migration path through Ontario followed by blackpolls with Central Region breeding origins is consistent with patterns of genetic structure in blackpoll populations. Ralston

and Kirchman (2012) found that close to 40% of variation in 77 haplotypes (287 individuals) was accounted for by a split between samples from far western populations (British Columbia, southwestern and southcentral Alaska) and samples from populations east of the Rocky Mountains. Within the latter group there was additional genetic structure. Samples from eastern Alaska and Canadian provinces from Alberta to Ontario showed haplotype affinity both with samples from west of the Rockies and from east of the Great Lakes. Samples from the Northwest Territories, however, shared no haplotypes with those from west of the Rockies, grouping only with samples from breeding sites east of the Great Lakes. Ralston and Kirchman (2012) suggested that the southeasterly fall migration route taken by blackpolls that breed in Alaska and Yukon largely passes south of the Northwest Territories, thereby restricting opportunities for genetic mixing between those regional populations. Our results indicate that mixing between these populations is restricted in spring migration as well, with blackpolls bound for the Northwest Territories sharing much of their route with birds breeding east of the Great Lakes. Additionally, we propose (see Fig. 7B) that spring migrants passing through the most southwesterly portion of the spring migration range within the United States are headed for northwestern Canada and Alaska, further separating the population in Alaska and British Colombia from that in eastern Northwest Territories.

More study is needed to verify the spring migration routes proposed in Fig. 7B. The growing network of Motus automated radio telemetry receivers across North America (Taylor et al. 2017) could be an important tool for such work, despite a shortage of receiving towers within the boreal breeding grounds, because coverage is now quite extensive across the United States. Radio tagging blackpolls captured in spring on the Gulf Coast and in Florida, combined with feather collection from the tagged individuals for stable isotope analysis, could help answer several key questions. For example, although blackpolls breeding in the Maritime provinces clearly follow a coastal route in spring that takes birds east of MGBO in Montreal, Motus detections could show how far inland that coastal migration corridor extends. Individual tracking would also test the validity of our hypothesized spring routes (Fig. 7B); a high priority because confirmation of longitudinal separation in the routes taken by spring migrants across the U.S.-Canada border would greatly enhance the value of spring migration counts for purposes of monitoring population change in different parts of western Canada and Alaska.

Temporal change in origins

Repeat sampling of δ^2H_f values in different years at several sites near the Great Lakes has revealed changes in catchment area over time. The spring routes described here are based largely on feather samples collected in 2007–2008 or later (Appendix 1), whereas earlier samples from TCBO and LPBO show that East Region birds were formerly more common there. A similar result was reported by Gómez et al. (2021), who found that feathers from blackpolls wintering in Colombia in 1972–1975 had δ^2H_f values indicating feathers were grown east of the Great Lakes, whereas feathers sampled in 2018–2019 were grown farther north and west, similar to the northwestward shifts we detected in catchment area for TCBO and LPBO. Although it is possible that δ^2H values in rainfall at the continental scale shifted over this period, it is unlikely to have caused the magnitude of changes observed in δ^2H_f values. Instead, dramatic shifts in δ^2H_f are likely to result from changes in breeding range or of migration routes without reductions in total population size and/or from differential population change among isotopic zones (Gómez et al. 2021). Both of these factors may have occurred in blackpolls. The Breeding Bird Survey indicates a decline of 75% in Canada since 1970, mostly attributable to decreases recorded in the Maritime Provinces and Quebec and with most of the decline taking place prior to 1980 (Sauer et al. 2020, Smith et al. 2023). Numbers of migrant blackpolls at MBO (Massachusetts) also decreased severely prior to 1980 (Lloyd-Evans and Atwood 2004). However, the striking loss of birds with δ^2H_f values indicating East Region origin from samples collected at LPBO between 2001 and 2015 (Fig. 4B) took place much later. Despite this change, blackpoll trends at LPBO both in spring and fall have remained stable or even increased slightly since counts began in 1960 (Birds Canada 2020), suggesting that any decline in abundance of Eastern Region migrants at LPBO is potentially being masked by increase in birds from farther west.

Conclusion

Our study improved resolution of population-specific spring and fall migratory pathways of Blackpoll Warblers within North America, using δ^2H assays of tail feathers and measurements of wing length, and provided the first quantitative estimates of migratory connectivity between breeding and migration routes for this species. Although sample sizes for δ^2H_f at individual capture sites were small, results revealed consistent geographic patterns at the continental scale, and geographic variation in wing length was consistent with assignments based solely on δ^2H_f.

This study serves as a template for defining migration pathways for additional boreal-breeding species. We have demonstrated that by first constraining the coarse spatial assignments based on feather isotopes using ancillary data collected at migration monitoring stations, hypotheses can be generated that are testable with strategic studies using more expensive technologies. Much can be learned from this approach about the origins, timing, routes, and shifts in regional composition of migrants at any particular stopover site (Hobson et al. 2014). Ultimately, identification of population-specific catchment areas and migration routes is needed for the modeling of population trends of migratory bird species not monitored effectively by existing breeding ground surveys, for interpreting the changes in the breeding ground origins of birds passing through specific migration sites, and for directing effective conservation action to all areas occupied throughout the year by populations of concern.

Author Contributions:

Equal contributions from primary authors: EHD (conceptualization, writing) and KJK (statistical analyses, writing). KMC, SRM, RLH, and KAH contributed throughout to data compilation, discussion, review, and editing.

Acknowledgments:

Hundreds of bird banders across North America have contributed to amassing the banding data sets and feather collections for stable isotope study that made this study possible. Our thanks to them as well as to those who helped us compile their data (Appendix 1). Access to wing length data collected by participants in the Monitoring Avian Productivity and Survival (MAPS) program was arranged by Danielle Kaschube and made possible by funding from the National Science Foundation (Grant EF 1703048). Additional wing length data for breeding birds were provided by Y. Aubry, R. Boardman, G. Campbell, L. McDuffie, P. Taylor, S. Savage, I. Warkentin, and D. Whitaker. Special thanks to Steve Van Wilgenburg for contributions during early stages of this paper. G. Koehler ran the isotope assays at the Environment and Climate Change Canada (ECCC) stable isotope laboratory in Saskatoon, Saskatchewan. We thank J. Hostetler for rapid bug fixes and guidance on using the MigConnectivity R library. Two anonymous reviewers provided feedback that greatly improved the manuscript. Funding for the stable isotope analyses was made through an operating grant by ECCC to K. A. Hobson.

LITERATURE CITED

Bazzi, G., A. Galimberti, Q. R. Hays, I. Bruni, J. G. Cecere, L. Gianfranceschi, K. A. Hobson, Y. E. Morbey, N. Saino, C. G. Guglielmo, and D. Rubolini. 2016. *Adcyap1* polymorphism covaries with breeding latitude in a Nearctic migratory songbird, the Wilson's warbler (*Cardellina pusilla*). Ecology and Evolution 6:3226-3239. https://doi.org/10.1002/ece3.2053

BirdLife International and NatureServe. 2014. Bird species distribution maps of the world. Version 2.0 BirdLife International, Cambridge, UK and NatureServe, Arlington, USA. https://datazone.birdlife.org/home

Birds Canada. 2023. Canadian Migration Monitoring Network. Data accessed from NatureCounts, a node of the Avian Knowledge Network, Birds Canada. http://www.naturecounts.ca/

Bivand, R. S, and C. Rundel. 2021. Rgeos: interface to Geometry Engine—Open Source ('GEOS'). Version 0.5-8. R Core Team, Vienna, Austria.

Bivand, R., T. Keit, and B. Rowlingson. 2023. rgdal: Bindings for the 'Geospatial' Data Abstraction Library. http://rgdal.r-forge.r-project.org, https://gdal.org, https://proj.org, https://r-forge.r-project.org/projects/rgdal/

Bowen, G. J., L. I. Wassenaar, and K. A. Hobson. 2005. Global application of stable hydrogen and oxygen isotopes to wildlife forensics. Oecologia 143:337-348. https://doi.org/10.1007/s00442-004-1813-y

Canadian Migration Monitoring Network. 2021. The Canadian Migration Monitoring Network—réseau Canadien de surveillance des migrations: researching Canada's landbirds for twenty years. CMMN-RCSM Scientific Technical Report no. 3. Birds Canada, Port Rowan, Ontario, Canada. https://birdscanada.org/wp-content/uploads/2022/01/CMMN_20YEARS_20220119.pdf

Cardenas-Ortiz, L., N. Bayly, and K. A. Hobson. 2021. Fuel loads of Neotropical migrant songbirds on autumn passage through the Darién region of Colombia: influence of migratory distance, route, ENSO, age and body size. Animal Migration 8:27-39. https://doi.org/10.1515/ami-2020-0105

Cohen, E. B., J. A. Hostetler, J. A. Royle, and P. P. Marra. 2014. Estimating migratory connectivity of birds when re-encounter probabilities are heterogeneous. Ecology and Evolution 4 (9):1659-1670. https://doi.org/10.1002/ece3.1059

Covino, K. M., S. R. Morris, M. Shieldcastle, and P. D. Taylor. 2020. Spring migration of Blackpoll Warblers across North America. Avian Conservation and Ecology 15(1):17. https://doi.org/10.5751/ACE-01577-150117

Crewe, T. L., J. D. McCracken, P. D. Taylor, D. Lepage, and A. E. Heagy. 2008. The Canadian Migration Monitoring Network—Reseau Canadien de surveillance des migrations: ten-year report on monitoring landbird population change. CMMN-RCSM Scientific Technical Report #1, Bird Studies Canada, Port Rowan, Ontario, Canada. https://www.bsc-eoc.org/download/CMMNReport2008.pdf

Delingat, J., K. A. Hobson, V. Dierschke, H. Schmaljohann, and F. Bairlein. 2011. Morphometrics and stable isotopes differentiate populations of Northern Wheatears (*Oenanthe oenanthe*). Journal of Ornithology 152:383-395. https://doi.org/10.1007/s10336-010-0599-4

DeLuca, W., R. Holberton, P. D. Hunt, and B. C. Eliason. 2020. Blackpoll Warbler (*Setophaga striata*), version 1. 0. In A. F. Poole, editor. Birds of the world. Cornell Lab of Ornithology, Ithaca, New York, USA. https://birdsoftheworld.org/bow/species/bkpwar/cur/introduction

DeLuca, W. V., B. K. Woodworth, S. A. Mackenzie, A. E. M. Newman, H. A. Cooke, L. M. Phillips, N. E. Freeman, A. O. Sutton, L. Tauzer, C. McIntyre, I. J. Stenhouse, S. Weidensaul, P. D. Taylor, and D. R. Norris. 2019. A boreal songbird's 20,000 km migration across North America and the Atlantic Ocean. Bulletin of the Ecological Society of America 100(3):1-5. https://doi.org/10.1002/bes2.1551

DeLuca, W. V., B. K. Woodworth, C. C. Rimmer, P. P. Marra, P. D. Taylor, K. P. McFarland, S. A. Mackenzie, and D. R. Norris. 2015. Transoceanic migration by a 12 g songbird. Biology Letters 11 (4): 20141045. https://doi.org/10.1098/rsbl.2014.1045

Dunn, E. H., B. L. Altman, J. Bart, C. J. Beardmore, H. Berlanga, P. J. Blancher, G. S. Butcher, D. W. Demarest, R. Dettmers, W. C. Hunter, et al. 2005. High priority needs for range-wide monitoring of North American landbirds. Partners in Flight Technical Series No. 2. Partners in Flight. https://www.partnersinflight.org/wp-content/uploads/2017/03/PIF-Technical-Series-02-Monitoring-Needs.pdf

Dunn, E. H., K. A. Hobson, L. I. Wassenaar, D. J. T. Hussell, and M. L. Allen. 2006. Identification of summer origins of songbirds migrating through southern Canada in autumn. Avian Conservation and Ecology — Écologie et conservation des oiseaux 1(2):4. https://doi.org/10.5751/ACE-00048-010204

Environment and Climate Change Canada (ECCC). 2019. Blackpoll Warbler. Status of Birds in Canada 2019. Environment

https://wildlife-species.canada.ca/bird-status/oiseau-bird-eng.aspx?sY=2019&sL=e&sM=a&sB=BLPW

Fink, D., T. Auer, A. Johnston, M. Strimas-Mackey, S. Ligocki, O. Robinson, W. Hochachka, L. Jaromczyk, A. Rodewald, C. Wood, I. Davies, and A. Spencer. 2022. eBird Status and Trends, Data Version: 2021; Released: 2022. Cornell Lab of Ornithology, Ithaca, New York, USA. https://doi.org/10.2173/ebirdst.2021

Flinks, H., and V. Salewski. 2012. Quantifying the effect of feather abrasion on wing and tail length measurements. Journal of Ornithology 153:1053-1065. https://doi.org/10.1007/s10336-012-0834-2

Fox, J., and S. Weisberg. 2019. An R companion to applied regression. Third edition. Sage, Thousand Oaks, California, USA. https://socialsciences.mcmaster.ca/jfox/Books/Companion/

Franzoi, A., S. Larsen, P. Franceschi, K. A Hobson, P. Pedrini, F. Camin, and L. Bontempo. 2021. Multidimensional natal isotopic niches reflect migratory patterns in birds. Scientific Reports 11:20800. https://doi.org/10.1038/s41598-021-00373-9

Gómez, C., K. A. Hobson, N. J. Bayly, K. V. Rosenberg, A. Morales-Rozo, P. Cardozo, and C. D. Cadena. 2021. Migratory connectivity then and now: a northward shift in breeding origins of a long-distance migratory bird wintering in the tropics. Proceedings of the Royal Society of London, Series B 288:20210188. https://doi.org/10.1098/rspb.2021.0188

Hijmans, R. 2023. raster: geographic data analysis and modeling. R package version 3.6-23. https://CRAN.R-project.org/package=raster

Hobson, K. A. 2019. Application of isotopic methods to track animal movements. Pages 85-116 in K. A. Hobson and L. I. Wassenaar, editors. Tracking animal migration using stable isotopes. Second edition. Academic Press, London, UK.

Hobson, K., S. L. Van Wilgenburg, E. Dunn, D. Hussell, P. Taylor, and D. Collister. 2015. Predicting origins of passerines migrating through Canadian migration monitoring stations using stable-hydrogen isotope analyses of feathers: a new tool for bird conservation. Avian Conservation and Ecology 10(1):3. https://doi.org/10.5751/ACE-00719-100103

Hobson, K. A., S. L. Van Wilgenburg, J. Faaborg, J. D. Toms, C. Rengifo, A. Llanes Sosa, Y. Aubry, and R. Brito Aguilar. 2014. Connecting breeding and wintering grounds of Neotropical migrant songbirds using stable hydrogen isotopes: a call for an isotopic atlas of migratory connectivity. Journal of Field Ornithology 85:237-257. https://doi.org/10.1111/jofo.12065

Hobson, K. A., S. L. Van Wilgenburg, L. I. Wassenaar, and K. Larson. 2012. Linking hydrogen (δ^2H) isotopes in feathers and precipitation: sources of variance and consequences for assignment to global isoscapes. PLoS ONE 7(4):e35137. https://doi.org/10.1371/journal.pone.0035137

Hobson, K. A. and Wassenaar, L I., editors. 2019. Tracking animal migration using stable isotopes. Second edition. Academic Press, London, UK.

Holberton, R. L., S. L. Van Wilgenburg, A. J. Leppold, and K. A. Hobson. 2015. Isotopic (δ^2H_f) evidence of "loop migration" and use of the Gulf of Maine flyway by both western and eastern breeding populations of Blackpoll Warblers. Journal of Field Ornithology 86(3):213-28. https://doi.org/10.1111/jofo.12112

Holberton, R. L., S. L. Van Wilgenburg, A. J. Leppold, and K. A. Hobson. 2019. Erratum: Isotopic ($\delta 2H_f$) evidence of "loop migration" and use of the Gulf of Maine flyway by both western and eastern breeding populations of Blackpoll Warblers. Journal of Field Ornithology 90(3):286-288. https://doi.org/10.1111/jofo.12305

Hostetler, J., and M. Hallworth. 2023. MigConnectivity: estimate migratory connectivity for migratory animals. R package version 0.4.2.

IAEA/WMO. 2020. Global network of isotopes in precipitation. The GNIP Database. https://nucleus.iaea.org/wiser.

Lloyd-Evans, T. L., and J. L. Atwood. 2004. 32 years of change in passerine numbers during spring and fall migrations in coastal Massachusetts. Wilson Bulletin 116:1-16. https://doi.org/10.1676/0043-5643(2004)116[0001:YOCIPN]2.0.CO;2

Ma, Y., B A. Branfireun, K. A. Hobson, and C. G. Guglielmo. 2018. Evidence of negative seasonal carry-over effects of breeding ground mercury exposure on survival of migratory songbirds. Journal of Avian Biology 49(3):e01656. https://doi.org/10.1111/jav.01656

Morris, S. R., K. M. Covino, J. D. Jacobs, and P. D. Taylor. 2016. Fall migratory patterns of the Blackpoll Warbler at a continental scale. Auk 133:41-51. https://doi.org/10.1642/AUK-15-133.1

Ożarowska, A., G. Zaniewicz, and W. Meissner. 2021. Sex and age-specific differences in wing pointedness and wing length in blackcaps *Sylvia atricapilla* migrating through the southern Baltic coast. Current Zoology 67:271-277. https://doi.org/10.1093/cz/zoaa065

Piranga. 2021. Piranga: a bird-bander's aid to identifying, ageing and sexing birds of the Western hemisphere. https://www.natureinstruct.org/piranga

Pyle, P. 1997. Identification guide to North American birds. Part 1, Columbidae to Ploceidae. Slate Creek Press, Bolinas, California, USA.

R Core Team. 2022. R: a language and environment for statistical computing. R Foundation for Statistical Computing. Vienna, Austria. https://www.r-project.org/

Ralph, C. J., G. R. Geupel, P. Pyle, P., T. E. Martin, and D. F. DeSante. 1993. Handbook of field methods for monitoring landbirds. USDA Forest Service General Technical Report PSW-144. Albany, New York, USA. https://doi.org/10.2737/PSW-GTR-144

Ralston, J., and J. J. Kirchman. 2012. Continent-scale genetic structure in a boreal forest migrant, the Blackpoll Warbler (*Setophaga striata*). Auk 129(3):467-78. https://doi.org/10.1525/auk.2012.11260

Ruegg, K. C., E. C. Anderson, K. L. Paxton, V. Apkenas, S. Lao, R. B. Siegel, D. F. DeSante, F. Moore, and T. B. Smith. 2014. Mapping migration in a songbird using high-resolution genetic markers. Molecular Ecology 23:5726-5739. https://doi.org/10.1111/mec.12977

Ruegg, K. C., and T. B. Smith. 2002. Not as the crow flies: a historical explanation for circuitous migration in Swainson's thrush (*Catharus ustulatus*). Proceedings of the Royal Society of London, Series B 269:1375-1381. https://doi.org/10.1098/rspb.2002.2032

Rushing, C. S., T. B. Ryder, J. F. Saracco, and P. P. Marra. 2014. Assessing migratory connectivity using multiple intrinsic markers. Ecological Applications 24(3):445-456. https://doi.org/10.1890/13-1091.1

Sauer, J.R., Link, W. A., and Hines, J. E., 2020, The North American Breeding Bird Survey, analysis results 1966 — 2019. U. S. Geological Survey data release. United States Geological Survey, Reston, Virginia, USA. https://doi.org/10.5066/P96A7675

Schmaljohann, H., J. W. Fox, and F. Bairlein. 2012. Phenotypic response to environmental cues, orientation and migration costs in songbirds flying halfway around the world. Animal Behaviour 84:623-640. https://doi.org/10.1016/j.anbehav.2012.06.018

Smetzer, J. R., and D. I. King. 2020. Intrinsic markers reveal breeding origin and geographically-structured migration timing of two songbird species at a coastal stopover site. Animal Migration 7:42-51. https://doi.org/10.1515/ami-2020-0005

Smith, A. C., Hudson, M-A. R. Aponte, V. I., English, W. B., and Francis, C. M. 2023. North American Breeding Bird Survey — Canadian Trends Website, Data-version 2021. Environment and Climate Change Canada, Gatineau, Quebec, Canada. https://wildlife-species.canada.ca/breeding-bird-survey-results/P001/A001/?lang=e

Smith, E. L., M. W. Reudink, P. P. Marra, A. E. McKellar, and S. L. Van Wilgenburg. 2019. Breeding origins and migratory connectivity at a northern roost of Vaux's Swift, a declining aerial insectivore. Condor 121:duz034. https://doi.org/10.1093/condor/duz034

Taylor, P. D., T. L. Crewe, S. A. Mackenzie, D. Lepage, Y. Aubry, Z. Crysler, G. Finney, C. M. Francis, C. G. Guglielmo, D. J. Hamilton, R. L. Holberton, P. H. Loring, G. W. Mitchell, D. Norris, J. Paquet, R. A. Ronconi, J. Smetzer, P. A. Smith, L. J. Welch, and B. K. Woodworth. 2017. The Motus Wildlife Tracking System: a collaborative research network to enhance the understanding of wildlife movement. Avian Conservation and Ecology 12(1):8. https://doi.org/10.5751/ACE-00953-120108

Vander Zanden, H. B, M. B. Wunder, K. A. Hobson, S. Van Wilgenburg, L. I. Wassenaar, J. M. Welker, and G. J. Bowen. 2014. Contrasting assignment of migratory organisms to geographic origins using long-term versus year-specific precipitation isotope maps. Methods in Ecology and Evolution 5:891-900. https://doi.org/10.1111/2041-210X.12229

Van Wilgenburg, S. L., and K. A. Hobson. 2011. Combining feather stable isotope (δD) and band recovery data to improve probabilistic assignment of migratory birds to origin. Ecological Applications 21:1340-1351. https://doi.org/10.1890/09-2047.1

Venables, W. N., and B. D. Ripley (2002). Modern applied statistics with S. Fourth edition. Springer, New York, New York, USA.

Wassenaar, L. I. 2019. Introduction to conducting stable isotope measurements for animal migration studies. Pages 25-51 in K. A. Hobson and L. I. Wassenaar, editors. Tracking animal migration with stable isotopes. Academic Press, London, UK.

Wassenaar, L. I., and K. A. Hobson. 2003. Comparative equilibration and online technique for determination of non-exchangeable hydrogen of keratins for use in animal migration studies. Isotopes in Environmental and Health Studies 39:211-217. https://doi.org/10.1080/1025601031000096781

Webster, M. S., and P. P. Marra. 2005. The importance of understanding migratory connectivity and seasonal interactions. Pages 199-209 in R. Greenberg and P. P. Marra, editors. Birds of two worlds: the ecology and evolution of migration. John Hopkins University Press, Baltimore, Maryland, USA.

Wunder, M. B. 2010. Using isoscapes to model probability surfaces for determining geographic origins. Pages 251-270 in G. J. Bowen, J. B. West, K. P. Tu, and T. E. Dawson, editors. Isoscapes: understanding movement, pattern, and process on earth through isotope mapping. Springer Netherlands, Dordrecht, Netherlands.

Editor-in-Chief: Judit K. Szabo
Subject Editor: Marc-André Villard

Sponsored by the Society of Canadian Ornithologists and Birds Canada

Parrainée par la Société des ornithologistes du Canada et Oiseaux Canada

Appendix 1. Sample sizes and sources for δ^2H_f and wing measurements from migration count sites.

Location name	Prov/ State	Migration site code	Latitude	Longitude	Isotope samples n spring/n fall	Year of feather samples	Wing chord n spring/ n fall	Contributor[1]
Creamer's Field Migration Station	AK	CFMS	64.86	-147.74			465/146	Claire Stuyck
Teslin Lake Bird Banding Station	YK	TLBBS	60.23	-132.92			-/140	Ben Schonewille, Ted Murphy-Kelly
Albert Creek Bird Observatory	YK	ACBO	60.06	-128.92	25/-	2007	566/76	Ben Schonewille, Ted Murphy-Kelly
Mackenzie Nature Observatory	BC	MNO	55.40	-123.21	-/29	1998-2001	2/89	Vi Lambie, David Lambie, CMMN
Lesser Slave Lake Bird Observatory	AB	LSLBO	55.41	-114.81			138/10	Patti Campsall
Inglewood Bird Observatory	AB	IBO	51.02	-114.01			65/22	Doug Collister
Last Mountain Lake	AB	LMBO	51.35	-105.22			171/283	Al Smith
South Dakota Game, Fish & Parks	SD[2]	SDGFP	44.55	-100.67			261/	Eileen Dowd Stukel
Delta Marsh Bird Observatory	MB	DMBO	50.18	-98.39	-/30	1998-2001	455/50	Paula Grieef, CMMN
Thunder Cape Bird Observatory	ON	TCBO	48.31	-88.93	-/56	1999 and 2007	86/85	Rinchen Boardman, CMMN
Pittsfield Bird Observatory	MI	PFBO	42.36	-85.59			7/253	Rich Keith
Black Swamp Bird Observatory	OH	BSBO	41.61	-83.19			1822/4962	Mark Shieldcastle
Pelee Island Bird Observatory	ON	PIBO	41.74	-82.68			25/75	Sumiko Onishi
Bruce Peninsula Bird Observatory	ON	BPBO	45.21	-81.42			29/35	Stéphane Menu
Long Point Bird Observatory	ON	LPBO	42.55	-80.25	54/81	2000, 2001, 2007, 2014, 2015	1634/4716	Stuart Mackenzie, Yanju Ma, CMMN
Cape Florida Banding Station	FL	CFBS	25.68	-80.16			297/14	Michelle Davis, Rebecca Holberton
Powdermill Avian Research Center	PA	PARC	40.16	-79.27	-/54	2007-2008	168/356	Luke De Groote
Presque Isle State Park	PA	PIPS	42.17	-80.11			233/-	Sarah Sargent
Haldimand Bird Observatory (Ruthven)	ON	RUTH	42.58	-79.52	10/-	2007	57/-	Rick Ludkin, CMMN
Tommy Thompson Park	ON	TTPBRS	43.63	-79.33	8/15	2007		CMMN
Braddock Bay Bird Observatory	NY	BBBO	43.32	-77.72			571/599	Andrea Patterson
Prince Edward Point Bird Obs	ON	PEPBO	43.94	-76.86	25/-	2007-2008	242/575	Nick Bartok, CMMN
Foreman's Branch Bird Observatory	MD	FBBO	39.22	-76.07			117/48	Maren Gimpel
First Landing State Park	VA	FLSP	36.92	-76.05			321/-	Bob Reilly
Innis Point Bird Observatory	ON	IPBO	45.42	-75.92			367/13	Bill Petrie
McGill Bird Observatory	PQ	MGBO	45.43	-73.94	9/-	2008	265/57	Simon Duval, CMMN
Block Island Banding Station	RI	BIBS	41.17	-71.58				Kim Gaffett, Steve Reinert
Kingston Wildlife Research Station	RI	KWRS	41.48	-71.51			-/158	Peter Paton
Appledore Island Migration Station	ME	AIMS	42.99	-70.62	22/-	2014	1898/172	Sara Morris, Kristen Covino
Manomet Bird Observatory	MA	MBO	41.80	-70.50	-/68	2007-2009	1118/1736	Trevor Lloyd-Evans, Evan Dalton
Metinic Island	ME	MEIS	43.89	-69.13	25/40	2011, 2013, 2014	23/15	Rebecca Holberton
Atlantic Bird Observatory	NS	ABO	43.40	-66.02	-/25	1998-2001	263/469	Phil Taylor
Cap Tourmente Nat'l Wildlife Area	PQ	RNCT	47.06	-70.80			-/25	Pierre-Alexandre Dumas
Louisiana Gulf Coast	LA[2]	LGC	29.45	-91.05			134/-	Frank Moore, Kristen Covino
Massachusetts tower kills	MA[2]	MASS	42.37	-71.24	-/28	c. 1970		Rebecca Holberton
Mississippi Barrier Islands	MS[2]	MBI	30.27	-88.90			267/-	Frank Moore, Kristen Covino
Wisconsin tower kills	WI[2]	WISC	44.77	-91.26	-/8	c. 1970		Rebecca Holberton

[1] 'CMMN' indicates isotope values provided by the Canadian Migration Monitoring Network

[2] Regional coordinates only

Appendix 2. Sample sizes of wing chord from breeding sites by state or province. See Acknowledgements for contributors.

State/Province	N
Alaska	279
Yukon Territory	62
British Colombia	116
Northwest Territories	6
Alberta	36
Manitoba	87
Quebec	415
Vermont	142
Maine	74
New Brunswick	53
Nova Scotia	4
Newfoundland	418

Appendix 3. Supplementary material.

Figure A3.1. Wing length distribution of breeding Blackpoll Warblers in three the three Regions defined in Figure 1. See Appendix 2 for sample locations.

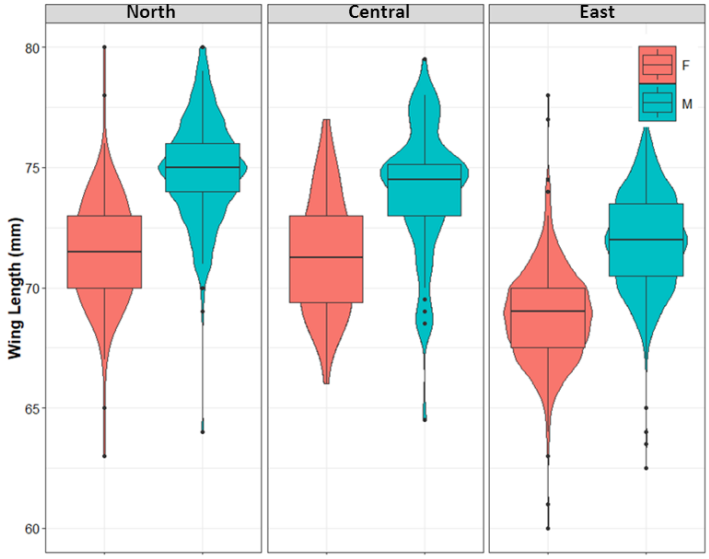

Figure A3.2. Coefficients of variation in 1000 bootstrapped assignments of δ^2H_f to the Breeding Regions defined in Figure 1.

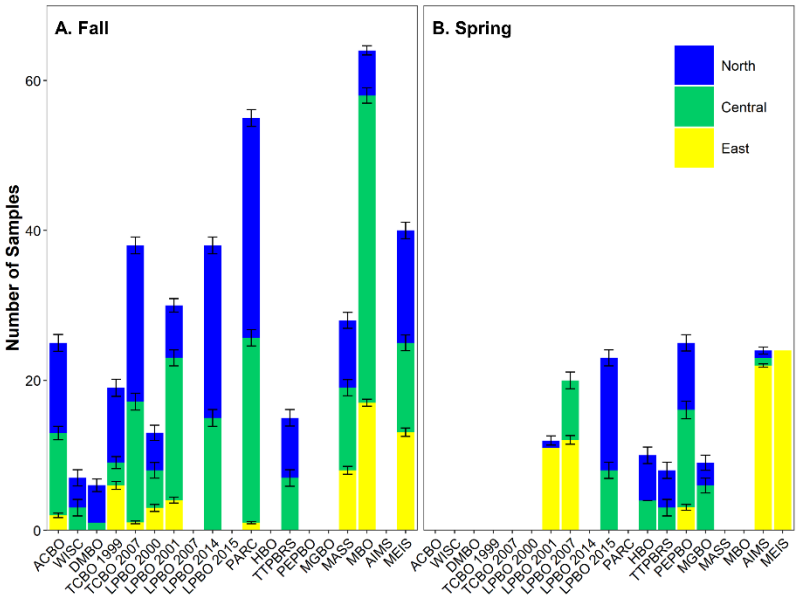

Figure A3.3. Geographic distribution of assigned breeding or natal origins of Blackpoll Warbler sampled during fall migration. The assignments included wing length as a Bayesian prior (see text). Red lines show the borders between the North, Central and East regions (Figure 1). The legend indicates probability from 0 to 1 (at top) that samples from the collection sites (indicated with red triangles) are isotopically consistent with a pixel of that color on the map. Assignment maps arranged west to east, with (n samples) following site name: A = Delta Marsh Bird Observatory (6), B = Wisconsin (8), C = Thunder Cape Bird Observatory (TCBO) in 1999 (21), D = TCBO in 2007 (38), E = Long Point Bird Observatory (LPBO) in 2000 (13), F = LPBO in 2001 (30), G) = LPBO in 2014 (38), H = (Powdermill Avian Research Center (54), I = Tommy Thompson Park Bird Research Station (15), J = Massachusetts (28), K = Manomet Bird Observatory (60), and L = Metinic Island (41).

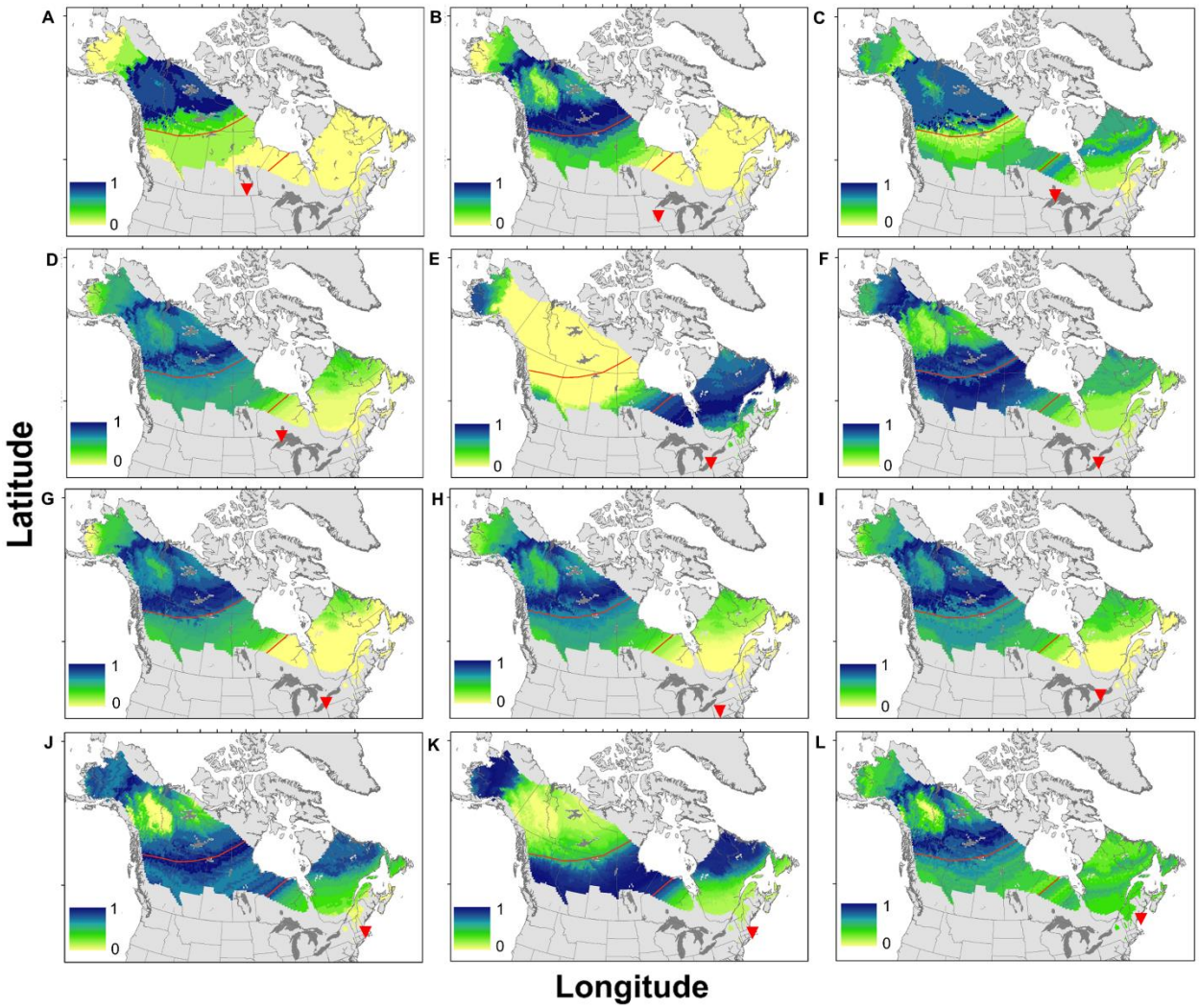

Figure A3.4. Geographic distribution of assigned breeding or natal origins of Blackpoll Warbler sampled during spring migration. Assignment includes Baysian prior for wing length. Red lines show the borders between the North, Central and East regions (Figure 1). The legend indicates probability from 0 to 1 (at top) that samples from the collection sites (indicated with red triangles) are isotopically consistent with a pixel of that color on the map. Assignment maps arranged west to east, with n samples following site name: A = Albert Creek Bird Observatory (25), B = Long Point Bird Observatory (LPBO) in 2001 (11), C = LPBO in 2007 (20), D = LPBO in 2015 (24), E = Haldimand Bird Observatory (10), F = (Tommy Thompson Park Bird Research Station (8), G = (Prince Edward Point Bird Observatory (25), H = McGill Bird Observatory (9), I = (Appledore Island Migration Station (23), and J = (Metinic Island (25).